Actin-dependence of the chloroplast cold positioning response in the liverwort *Marchantia polymorpha* L

Shun Kimura [1] , **Yutaka Kodama** Corresp. [1]

[1] Center for Bioscience Research and Education, Utsunomiya University, Utsunomiya, Tochigi, Japan

Corresponding Author: Yutaka Kodama
Email address: kodama@cc.utsunomiya-u.ac.jp

The subcellular positioning of chloroplasts can be changed by alterations in the environment such as light and temperature. For example, in leaf mesophyll cells, chloroplasts localize along anticlinal cell walls under high-intensity light, and along periclinal cell walls under low-intensity light. These types of positioning responses are involved in photosynthetic optimization. In light-mediated chloroplast positioning responses, chloroplasts move to the appropriate positions in an actin-dependent manner, although some exceptions also depend on microtubule. Even under low-intensity light, at low temperature (e.g., 5°C), chloroplasts localize along anticlinal cell walls; this phenomenon is termed chloroplast cold positioning. In this study, we analyzed whether chloroplast cold positioning is dependent on actin filaments and/or microtubules in the liverwort *Marchantia polymorpha* L. When liverwort cells were treated with drugs for the de-polymerization of actin filaments, chloroplast cold positioning was completely inhibited. In contrast, chloroplast cold positioning was not affected by treatment with a drug for the de-polymerization of microtubules. These observations indicate the actin-dependence of chloroplast cold positioning in *M. polymorpha*. Actin filaments during the chloroplast cold positioning response were visualized by using fluorescent probes based on fluorescent proteins in living liverwort cells, and thus, their behavior during the chloroplast cold positioning response was documented.

1   **Actin-dependence of the chloroplast cold positioning response in the liverwort *Marchantia***

2   ***polymorpha* L.**

3

4   Shun Kimura and Yutaka Kodama

5

6   Center for Bioscience Research and Education, Utsunomiya University, Utsunomiya, Tochigi

7   321-8505, Japan

8

9   Corresponding author:

10   Yutaka Kodama

11   350 Mine-machi, Utsunomiya, Tochigi 321-8505, Japan

12   E-mail address: kodama@cc.utsunomiya-u.ac.jp

13

14   **Abstract:**

15   The subcellular positioning of chloroplasts can be changed by alterations in the environment

16   such as light and temperature. For example, in leaf mesophyll cells, chloroplasts localize along

17   anticlinal cell walls under high-intensity light, and along periclinal cell walls under low-intensity

18   light. These types of positioning responses are involved in photosynthetic optimization. In light-

19   mediated chloroplast positioning responses, chloroplasts move to the appropriate positions in an

20   actin-dependent manner, although some exceptions also depend on microtubule. Even under

21   low-intensity light, at low temperature (e.g., 5°C), chloroplasts localize along anticlinal cell

22   walls; this phenomenon is termed chloroplast cold positioning. In this study, we analyzed

23   whether chloroplast cold positioning is dependent on actin filaments and/or microtubules in the

24   liverwort *Marchantia polymorpha* L. When liverwort cells were treated with drugs for the de-

25   polymerization of actin filaments, chloroplast cold positioning was completely inhibited. In

26   contrast, chloroplast cold positioning was not affected by treatment with a drug for the de-

27   polymerization of microtubules. These observations indicate the actin-dependence of chloroplast

28   cold positioning in *M. polymorpha*. Actin filaments during the chloroplast cold positioning

29   response were visualized by using fluorescent probes based on fluorescent proteins in living

30   liverwort cells, and thus, their behavior during the chloroplast cold positioning response was

31   documented.

32

33 **Introduction**

34 Chloroplasts change their subcellular localization in response to alterations in the environment

35 such as ambient light and temperature (Senn, 1908). In the light-mediated response of leaf

36 mesophyll cells, under high-intensity (strong) light conditions, chloroplasts localize along

37 anticlinal cell walls due to avoidance from the strong light (avoidance response). In contrast,

38 under low-intensity (weak) light conditions, chloroplasts localize along periclinal cell walls due

39 to accumulation to the weak light (accumulation response). Dark-induced positioning is also

40 known; for instance, chloroplasts localize to the bottom of cells in flowering plants such as

41 *Arabidopsis thaliana* (Suetsugu et al., 2005), and along the anticlinal cell walls in the liverwort

42 *Marchantia polymorpha* (Komatsu et al., 2014), and the fern *Adiantum capillus-veneris* (Kagawa

43 & Wada, 1996). Chloroplast positions also change with temperature alterations. When the

44 temperature was shifted from room temperature (e.g., 20°C) to low temperature (e.g., 5°C),

45 chloroplasts re-localize from periclinal cell walls to anticlinal cell walls, even if under weak light

46 conditions. Over one century ago, cold-induced chloroplast relocation movements (cold

47 positioning) were analyzed in the moss *Funaria hygrometrica* (Senn, 1908). Recently, we also

48 found that cold positioning occurs in the ferns *A. capillus-veneris* and *Pteris cretica* as well as

49 the liverwort *M. polymorpha* (Kodama et al., 2008; Ogasawara et al., 2013). Although a blue-

50 light photoreceptor, phototropin2, was reported to mediate chloroplast cold positioning in *A.*

51 *capillus-veneris* (Kodama et al., 2008), other factors involved in cold positioning have not been

52 found.

53   It is well known that actin cytoskeletal filaments are involved in light-induced chloroplast

54 positioning (Gabryś, 2004; Wada & Suetsugu, 2004; Suetsugu & Wada, 2007; Kong & Wada,

55 2011). The anti-actin drugs (actin polymerization inhibitors) such as cytochalasin and latrunculin,

56 which depolymerize actin filaments, prevent light-induced chloroplast positioning in green alga

57 and vascular plants (Wagner, Haupt & Laux, 1972; Malec, Rinaldi & Gabryś, 1996; Kandasamy

58 & Meagher, 1999). Recently, in a study of light-induced chloroplast positioning, short actin

59 filaments were found on the chloroplast periphery in transgenic *A. thaliana* expressing a

60 genetically encoded fluorescent probe (GFP-mTalin) that binds to actin filaments (Kadota et al.,

61 2009). The short actin filaments are now called chloroplast actin (cp-actin) filaments. Cp-actin

62 filaments evenly distribute at the periphery of unmoving chloroplasts; they reorganize on the

63 chloroplast in response to light before and during relocation with a biased distribution of cp-actin

64 filaments at the front region of the chloroplast (Kadota et al., 2009). Cp-actin filaments exhibit

65 rapid dynamic changes during light-induced chloroplast positioning (Kadota et al., 2009; Kong et

66 al., 2013), therefore, they seem to be an important machinery in the light-induced chloroplast

67 positioning observed in *A. thaliana* (Kadota et al., 2009), *A. capillus-veneris* (Tsuboi & Wada,

68 2012) and *P. patens* (Yamashita et al., 2011). In *P. patens*, an involvement of microtubules in

69 addition to actin filaments has been reported in light-induced chloroplast positioning (Sato,

70 Wada & Kadota, 2001). When *P. patens* is exposed to the anti-microtubule drug (microtubule

71 polymerization inhibitor) Cremart, the red-light-induced chloroplast positioning response was

72 completely inhibited (Sato, Wada & Kadota, 2001). Blue-light-induced chloroplast positioning in

73 *P. patens* was partially inhibited by Cremart, and completely inhibited by simultaneous treatment

74 of Cremart and cytochalasin B (Sato, Wada & Kadota, 2001). However, the molecular

75 mechanism of temperature-dependent chloroplast positioning is not completely understood, and

76 it is unknown whether the chloroplast cold positioning response is mediated via cytoskeletal

77 filaments such as actin and/or microtubules.

78   In this study, we used de-polymerization drugs and cytoskeletal filament fluorescent probes

79   to determine whether chloroplast cold positioning is dependent on actin filaments and/or

80   microtubules in the liverwort *M. polymorpha*.

81

82   **Materials and Methods**

83   **Plant materials and growth conditions**

84   The male strain (Tak-1) of *M. polymorpha* was used in this study. As previously described

85   (Ogasawara et al., 2013), the thalli were cultured on M51C medium with 1% agar (M51C agar),

86   and asexually maintained under 75 µmol photons m^{-2} s^{-1} continuous white light (FL40SW, NEC

87   Corporation, Tokyo, Japan). One-day-old gemmalings (immature thalli grown from gemmae)

88   obtained from approximately 1-month-old wild type or transgenic thalli (G1 generation) were

89   used for all experiments.

90

91   **Treatments of temperature, light, and inhibitors**

92   One-day-old gemmalings were incubated at 22°C or 5°C in the temperature-controlled

93   incubators (IJ100 or IJ101, Yamato Scientific Co., Ltd., Tokyo, Japan). In the incubators,

94   illuminators with white- or blue-colored light-emitting diodes (LEDs) (OptoSupply Limited,

95   Hong Kong, China) were set-up to irradiate the gemmalings with weak light (Ogasawara et al.,

96   2013; Fujii and Kodama et al., in preparation). The gemmalings were incubated at 22°C for 2 h

97   followed by transfer at 5°C for 24 h to induce chloroplast cold positioning.

98   Before induction of chloroplast cold positioning, inhibitors (1-µM latrunculin A, 50-µM

99   cytochalasin B, or 10-µM oryzalin) were applied at 22°C for 2 h. To prepare the drugs with

100   appropriate concentrations for use, stock solutions stored at −20°C were diluted with sterile

101   water. The stock solutions were 0.1-mM latrunculin A in ethanol, 20-mM cytochalasin B in

102   dimethyl sulfoxide (DMSO) protected from light, and 10-mM oryzalin in DMSO protected from

103   light.

104   For analysis of chloroplast accumulation response, dark positioning response of chloroplast

105   was induced under dark at 22°C for 4 days, and then the cells were treated with an inhibitor, 1-

106   μM latrunculin A or 10-μM oryzalin, under the dark at 22°C for 2 h. The treated cells were

107   transferred to weak blue-light (25 μmol photons m^{-2} s^{-1}) condition and incubated for 12 h to

108   induce chloroplast accumulation response. For analysis of chloroplast avoidance response,

109   chloroplast accumulation response was induced under weak blue-light (25 μmol photons m^{-2} s^{-1})

110   condition at 22°C for 24 h, and the cells were treated with an inhibitor, 1-μM latrunculin A or

111   10-μM oryzalin, under the weak light condition at 22°C for 2 h. The treated cells were

112   transferred to strong blue-light (50 μmol photons m^{-2} s^{-1}) condition and incubated for 3 h to

113   induce chloroplast avoidance response.

114

115   **Plasmid constructions**

116   To visualize actin filaments and microtubules in *M. polymorpha*, binary vectors adapted to the

117   gateway cloning system (Invitrogen, CA, USA) (Ishizaki et al., 2015a) were used to perform

118   *Agrobacterium*-mediated transformations.

119   For Lifeact-Citrine, the cDNA fragment for the Lifeact peptide [MGVADLIKKFESISKEE]

120   (Riedl et al., 2008) was produced by PCR with the following oligo primers: [5′-

121   GGGGACAAGTTTGTACAAAAAAGCAGGCTTCATGGGCGTGGCCGACCTGATCAAGA

122   AGTTCGAGAGCATC-3′   and   5′-

123   ACCTCCAGAGCCACCCTCCTCCTTGCTGATGCTCTCGAACTT-3′]. The cDNA fragment

124   for Citrine was amplified by PCR with pDONR207-Citrine (Tsuboyama & Kodama, 2014) as a

125 template with the following oligo primers: [5′-

126 GGTGGCTCTGGAGGTATGGTGAGCAAGGGC-3′ and 5′-

127 GGGGACCACTTTGTACAAGAAAGCTGGGTCTCACTTGTACAGCTCGTCC-3′]. The two

128 fragments for Lifeact and Citrine were mixed, and this solution was then used as a template for

129 the second PCR to fuse the two fragments with the following oligo primers: [5′-

130 GGGGACAAGTTTGTACAAAAAAGCAGGCTTCATGGGCGTGGCCGACCTGATCAAGA

131 AGTTCGAGAGCATC-3′ and 5′-

132 GGGGACCACTTTGTACAAGAAAGCTGGGTCTCACTTGTACAGCTCGTCC-3′]. The

133 resulting fusion fragment for Lifeact-Citrine was cloned into the pDONR207 plasmid using the

134 BP reaction, and the sequence was checked. There is no linker sequence between Lifeact and

135 Citrine. The fusion gene for Lifeact-Citrine was transferred into pMpGWB403 (Ishizaki et al.,

136 2015a).

137　　　To construct the fusion gene for Citrine-mTalin, the cDNA fragment for mTalin was

138 amplified by PCR with a template DNA containing the cDNA of mTalin with the following

139 oligo primers: [5′-

140 GGGGACAAGTTTGTACAAAAAAGCAGGCTTCAGCGGAGCAGGAGCAGGA-3′ and 5′-

141 GGGGACCACTTTGTACAAGAAAGCTGGGTCTTAGTGCTCGTCTCGAAGC-3′]. The

142 amplified fragment was cloned into the pDONR207 plasmid using the BP reaction, and the

143 sequence was confirmed. The cloned gene for mTalin was transferred into the pMpGWB105

144 vector (Ishizaki et al., 2015a), which harbors the *Citrine* gene, generating a *Citrine-mTalin*

145 fusion gene. The amino acid sequence of a linker between Citrine and mTalin is

146 [AVITSLYKKAGF].

147　　　For visualization of microtubules, the cDNA fragment for MpTubulin beta 3 (accession

148 number: KJ948117) (Buschmann et al., 2016) was amplified by PCR with the cDNA library as a

149 template using the following oligo primers: [5′-

150 GGGGACAAGTTTGTACAAAAAAGCAGGCTTCATGAGAGAAATTCTCCAC-3′ and 5′-

151 GGGGACCACTTTGTACAAGAAAGCTGGGTCTTAGTTGGCTTCAAGCTCT-3′]. The

152 cDNA library prepared from the *M. polymorpha* Tak-1 strain was used. The amplified cDNA

153 fragment for MpTubulin was cloned into the pDONR207 plasmid using the BP reaction. After

154 the sequence was checked, the fragment was transferred into the pMpGWB105 vector (Ishizaki

155 et al., 2015a), which harbors the *Citrine* gene, generating a *Citrine-MpTubulin* fusion gene. The

156 amino acid sequence of a linker between Citrine and MpTubulin is [AVITSLYKKAGF].

157

158 **Genetic transformation of *Marchantia polymorpha***

159 *Agrobacterium*-mediated genetic transformation of *M. polymorpha* was performed by G- and T-

160 AgarTrap procedures (Tsuboyama-Tanaka & Kodama, 2015; Tsuboyama-Tanaka, Nonaka &

161 Kodama, 2015). In this study, Tak-1 was used as the material to produce these transformants. For

162 all experiments, transgenic G2 gemmae were used. Several transformants were independently

163 produced for each construct (*Lifeact-Citrine*, *Citrine-mTalin* or *Citrine-MpTubulin*), and it was

164 confirmed that the chloroplast cold positioning response was normally induced in these

165 transformants.

166

167 **Microscopic observation and analysis**

168 Observation of chloroplast position in gemmaling under a stereo fluorescence microscope using

169 an MZ16F system (Leica microsystems, Wetzlar, Germany) has been reported previously

170 (Ogasawara et al., 2013). Excitation filter 480/40 nm and barrier filter LP 510 nm were used for

171 observation, and the P/A ratio method (Kodama et al., 2008; Ogasawara et al., 2013) was utilized

172 for evaluation of chloroplast positioning in *M. polymorpha*. Because procedure of the P/A ratio

173 method for *M. polymorpha* was previously reported (Ogasawara et al., 2013), we briefly describe

174 in this paper. Chloroplast position was quantified by the brightness ratio of chlorophyll

175 fluorescence from chloroplasts along the anticlinal and periclinal cell walls. Fluorescent

176 intensities from 30 points (0.625 mm each) and 30 areas (39.1 mm^2 each) were measured along

177 the anticlinal and periclinal cell walls, respectively. After subtraction of background fluorescence

178 from each of the averaged fluorescent intensities, the P/A ratio with a standard deviation was

179 obtained as an average of experiments repeated five times (the raw data in Supplemental

180 Information).

181   To visualize the fluorescence of Lifeact-Citrine and Citrine-mTalin for actin filaments and

182 Citrine-MpTubulin for microtubules, a confocal laser scanning microscope SP8X system (Leica

183 microsystems, Wetzlar, Germany) was used with a 514-nm laser obtained from a highly flexible

184 pulsed white-light laser. Citrine and chlorophyll fluorescence were detected by the hybrid

185 detector and the conventional photomultiplier tube, respectively (Kodama, 2016). To reject

186 chlorophyll autofluorescence when Citrine fluorescence was observed, the time-gated imaging

187 method (Kodama, 2016) was employed with a gating time set at 0.5–12.0 ns. For capturing

188 images, the scan speed was set at 100 Hz (100 lines/s) and line averages were four times. To

189 visualize the fluorescence of Citrine in the nucleus and peroxisomes (Ogasawara et al., 2013),

190 another confocal laser scanning microscope SP2 system (Leica microsystems, Wetzlar,

191 Germany) was used with a 514-nm laser (Argon laser).

192

193 **Results and Discussion**

194   **Effects of inhibitors for cytoskeletal filaments in *M. polymorpha***

195   To determine whether chloroplast cold positioning is dependent on actin filaments and/or

196   microtubules, we treated gemmalings (thallus grown from gemma) with anti-actin and anti-

197   microtubule drugs, and observed the chloroplast cold positioning response in the cells. The

198   degree of the response was evaluated by the P/A ratio method, which is a quantitative method for

199   chloroplast positioning (Kodama et al., 2008; Ogasawara et al., 2013). Chloroplast position was

200   quantified by the brightness ratio of chlorophyll fluorescence from chloroplasts along the

201   anticlinal and periclinal cell walls, and chloroplast position was stated as the numeric value, P/A

202   ratio. A procedure of the P/A ratio method for *M. polymorpha* was previously reported

203   (Ogasawara et al., 2013).

204   To analyze the involvement of actin filaments in chloroplast cold positioning, 1-day-old

205   gemmalings cultured at 22°C for 24 h were pre-treated with 1-µM latrunculin A, an anti-actin

206   drug, at 22°C for 2 h followed by incubation at 5°C for 24 h to induce cold positioning (Fig. 1a).

207   The disruption of actin filaments with 1-µM latrunculin A was evaluated (see Figs. 3b, 3d, 4b,

208   and 4c). In the control experiment with 1% ethanol, cold positioning was typically induced (Fig.

209   1b), and the average P/A ratio changed from 1.2 at 22°C to 0.3 at 5°C (Fig. 1c). Conversely, in

210   the gemmalings treated with 1-µM latrunculin A, cold positioning was not induced (Fig. 1b), and

211   the average P/A ratio remained unchanged at 22°C and 5°C (Fig. 1c). To avoid unforeseen side

212   effects of latrunculin A, another anti-actin drug (cytochalasin B) was also tested. Disruption of

213   the actin filaments with 50-µM cytochalasin B was also confirmed in *M. polymorpha* (see Figs.

214   3b, 3d, 4b, and 4c). When 1-day-old gemmalings were pre-treated with 50-µM cytochalasin B at

215   22°C for 2 h (Fig. 1a), cold positioning was completely inhibited (Figs. 1b and 1c). In the control

216   experiment with 0.25% dimethyl sulfoxide (DMSO), we successfully observed the induction of

217 cold positioning (Figs. 1b and 1c). These results indicate that the induction of the chloroplast

218 cold positioning response is dependent on actin filaments in *M. polymorpha*. Our previous study

219 reported that, in addition to chloroplasts, the nucleus and peroxisomes also change their

220 subcellular localization in response to cold temperatures (Kodama et al., 2008; Ogasawara et al.,

221 2013). Transformants of *M. polymorpha*, wherein the nuclei or peroxisomes are visualized by

222 fluorescent proteins, have been previously produced (Ogasawara et al., 2013). In this study, the

223 transformants were treated with 1-µM of the anti-actin drug latrunculin A. Similar to

224 chloroplasts, latrunculin A inhibited cold-induced relocations of the nucleus and peroxisomes in

225 *M. polymorpha* (Figs. 1d and 1e); thus, cold-induced organelle relocation appears to be mediated

226 via actin filaments in *M. polymorpha*. Because light-induced positioning responses of nuclei and

227 peroxisomes are dependent on light-induced positioning responses of the attached chloroplasts

228 (Higa et al., 2014; Oikawa et al., 2015), the cold-induced relocations of the nuclei and

229 peroxisomes might be dependent on the relocation of the chloroplasts in *M. polymorpha*.

230   We next examined the effect of the anti-microtubule drug oryzalin on cold positioning (Fig.

231 2a). When transgenic gemmalings expressing Citrine-MpTubulin (Fig. 2b) were pre-treated with

232 10-µM oryzalin, disruption of microtubules was observed (Fig. 2c). MpTubulin-fused

233 fluorescent protein has been previously reported to visualize microtubules in *M. polymorpha*

234 (Buschmann et al., 2016). Note that the previous study used β-tubulin 1 from *M. polymorpha*,

235 while we employed β-tubulin 3 from *M. polymorpha* (Buschmann et al., 2016). Treatments

236 with oryzalin did not affect the cold positioning responses of chloroplasts (Figs. 2d and 2e), the

237 nucleus or peroxisomes (Fig. 2f), indicating no involvement of microtubules in the cold

238 positioning response.

239   Because microtubule is known to be cold sensitive (Hardham & Gunning, 1978), we

240   investigated the behavior of microtubule in *M. polymorpha*. In transgenic gemmalings

241   expressing Citrine-MpTubulin, cold-induced disruption of microtubules was observed after cold

242   treatment for 2 h (Fig. 2g), suggesting no formation of microtubules during chloroplast cold

243   positioning. In other words, disruption of microtubules may trigger to induce the relocation of

244   chloroplast from periclinal to anticlinal cell walls. However, oryzalin-induced disruption did not

245   change chloroplast positioning, although we observed for 24 h at 22°C (Fig. 2h). Taken together,

246   we concluded that microtubule is not involved in the chloroplast cold positioning response in *M.*

247   *polymorpha*.

248

249   **Visualization of actin filaments during chloroplast cold positioning**

250   Based on the above pharmacological experiments, the induction of the chloroplast cold

251   positioning response is dependent on actin filaments, but not microtubules, in *M. polymorpha*.

252   During the light-induced chloroplast positioning in *A. thaliana, A. capillus-veneris*, and *P. patens*,

253   the short cp-actin filaments that exhibit rapid dynamic changes on the chloroplast envelope were

254   reported (Kadota et al., 2009; Yamashita et al., 2011; Tsuboi & Wada, 2012; Kong et al., 2013).

255   To understand the behavior of actin filaments during cold positioning, actin filaments were

256   visualized by using genetically encoded fluorescent probes in *M. polymorpha*. The Lifeact

257   peptide, which is a short peptide of 17 amino acids known to bind to filamentous actin (F-actin)

258   (Riedl et al., 2008), was previously reported to visualize actin filaments by fusing with a

259   fluorescent protein in *M. polymorpha* (Era et al., 2009). In this study, we fused the Lifeact

260   peptide with the yellow fluorescent protein Citrine (Lifeact-Citrine) (Fig. 3a) and transformed

261   the fusion gene for Lifeact-Citrine into *M. polymorpha*. When 1-day-old transgenic gemmalings

262   expressing the Lifeact-Citrine were observed at 22°C, many chloroplasts localized along

263   periclinal cell walls, inducing the accumulation response (Fig. 3b). A network of long F-actin

264   structures was slightly observed in the 1-day-old cells (Fig. 3b), and clearly observed in the 4-

265   day-old cells (Fig. 3c). The structures were disrupted by anti-actin drugs (1-µM latrunculin A

266   and 50-µM cytochalasin B), verifying the visualization of F-actin (Fig. 3d). However, around the

267   chloroplasts in *M. polymorpha*, a liquid-like signal rather than a filamentous signal of Lifeact-

268   Citrine was observed, and a cp-actin-like structure was not detected (Figs. 3b and 3c). When cold

269   positioning was induced, the chloroplasts relocated from periclinal to anticlinal cell walls and the

270   long F-actin structures at periclinal cell walls were reduced together with the chloroplasts (Fig.

271   3b). Eventually, we could not observe cp-actin-like structures around the chloroplast during the

272   cold positioning response (Fig. 3b).

273   A previous study of *A. thaliana* demonstrated that mouse talin (mTalin) (Kost, Spielhofer &

274   Chua, 1998), which is another actin binding protein, is suitable for the visualization of cp-actin

275   as compared with the Lifeact peptide (Kong et al., 2013). In the moss *P. patens*, cp-actin

276   filaments have been successfully visualized by the mTalin-fused fluorescent protein (Yamashita

277   et al., 2011). Therefore, mTalin was considered to be suitable for observing cp-actin filaments.

278   We fused mTalin with Citrine (Citrine-mTalin) (Fig. 4a) and transformed Citrine-mTalin into *M.*

279   *polymorpha* (Fig. 4b). Surprisingly, the actin filaments visualized by Citrine-mTalin were totally

280   different from that by Lifeact-Citrine in the 1-day-old cells (Figs 3b and 4b), and numerous long

281   F-actin structures were clearly observed in the transgenic cells expressing Citrine-mTalin (Fig.

282   4b). In this context, a type of F-actin bound by Citrine-mTalin may differ from that bound by

283   Lifeact-Citrine. In addition, the structure was disrupted by anti-actin drugs (1-µM latrunculin A

284   and 50-µM cytochalasin B), visualizing F-actin with Citrine-mTalin (Fig. 4c). In the 1-day-old

285   transgenic gemmalings expressing the Citrine-mTalin, the chloroplast accumulation response

286 was induced at 22°C, and the long F-actin structures were visualized as likely covering the

287 chloroplasts (Fig. 4b). However, as with the case of Lifeact-Citrine (Fig. 3b), cp-actin-like short

288 F-actin structures were not detected by Citrine-mTalin (Fig. 4b). When cold positioning was

289 induced, any biased distribution of the actin filaments between the front and rear of chloroplasts

290 in its directional movement was also undetectable (Fig. 4b). However, the reduction of the long

291 F-actin structures at periclinal cell walls was clearly observed during chloroplast relocation in the

292 transgenic liverworts expressing Citrine-mTalin, confirming the results with Lifeact-Citrine (Fig.

293 4b).

294   In the present study, by using Lifeact-Citrine and Citrine-mTalin as fluorescent probes, we

295 detected long F-actin structures, but not short F-actin structures, such as cp-actin filaments,

296 around chloroplast in *M. polymorpha*. It remains to be known why these particular structures of

297 cp-actin were not detected in *M. polymorpha*. It is possible that the actin-based machinery

298 involved in the chloroplast positioning observed in *M. polymorpha* may differ from the already

299 reported cp-actin filaments as cp-actin-independent but actin-mediated mechanisms for light-

300 induced positioning have recently been suggested (Suetsugu et al., 2016). As a possibility, cp-

301 actin filaments may not form in chloroplast cold positioning. Based on our observations (Figs 3b

302 and 4b), long F-actin structures at periclinal cell walls may be involved in chloroplast cold

303 positioning of *M. polymorpha* but further experiments are necessary to make this conclusion.

304   Cp-actin filaments for chloroplast positioning have been found not only in the vascular

305 plants, *A. thaliana* (the flowering plant) and *A. capillus-veneris* (the fern), but also in a bryophyte

306 *P. patens* (the moss), and factors regulating cp-actin filaments are conserved in streptophytes

307 (Suetsugu and Wada 2016). Thus, the cp-actin filaments are believed to be conserved in many

308 plants including *M. polymorpha*. Actually, the light-induced chloroplast positioning responses

309   were dependent on actin filaments, but not microtubules, in *M. polymorpha* (Fig. 5). In our

310   microscopic observation and P/A ratio evaluation, both light-induced chloroplast avoidance and

311   accumulation responses were inhibited by latrunculin A, but not oryzalin (Fig. 5). Even if *M.*

312   *polymorpha* has chloroplast positioning responses via regulation by cp-actin filaments, the

313   structure would be different from the already reported cp-actin structure because there were no

314   observations of analogous structure at both 22°C and 5°C in the present study (Figs 3b and 4b).

315   In order to determine this in *M. polymorpha*, particularly during temperature-induced chloroplast

316   positioning responses, technical limitations of microscopic observation need to be overcome. In

317   the previous study of *A. thaliana*, to analyze the light-induced response, cp-actin was observed

318   by taking photographs (i.e., snapshot), and also by recording movies (i.e., time-lapse) (Kadota et

319   al., 2009). In the recoded movie of the light-induced response, both imaging and microbeam

320   irradiation were simultaneously performed (Kadota et al., 2009). In the present study, to analyze

321   temperature-induced responses, we took only photographs because technically it was not

322   possible to record movies with fluorescence images under cold conditions. In our experiments,

323   cells were observed by confocal laser scanning microscopy after temperature treatment in a

324   conventional incubator, suggestive of a time-lag (within minutes) between the treatment and the

325   observation. The reorganization of cp-actin filaments has been reported to occur on a minute

326   time-scale (Kadota et al., 2009), thus cp-actin filaments may have already disappeared in the

327   cells when they were scanned in our study. To find the expected cp-actin filaments under

328   temperature alteration, the use of temperature-controlled fluorescence microscopy or confocal

329   microscope equipped with a time-lapse video recording system may be necessary. Fluorescence

330   observation by confocal laser scanning microscopy under temperature controlled conditions has

331   been reported previously (Holzinger et al., 2007), thus these technical limitations should be

332   resolved in the future by adding a time-lapse recording system.

333   In summary, our findings indicate that chloroplast cold positioning is actin-dependent;

334   however, the actin-based machinery (i.e., cp-actin-like machinery associated with chloroplasts or

335   long F-actin structures along periclinal cell walls) necessary for the cold positioning response of

336   *M. polymorpha* could not be conclusively identified in the present study. Future work will

337   include temperature-controlled fluorescence microscopy with a time-lapse video recording

338   system to determine the machinery. Currently, *M. polymorpha* is being developed as a model

339   liverwort, and various molecular biological techniques such as transformation and genome

340   editing have been developed (Ishizaki et al., 2015b). We believe that future research using these

341   molecular techniques, in addition to temperature-controlled fluorescence microscopy, will allow

342   the identification of the actin-based machinery critical for the cold positioning response.

343

352

353   **References**

354   Buschmann H., Holtmannspötter M., Borchers A., O'Donoghue MT., Zachgo S. 2016.

355   Microtubule dynamics of the centrosome-like polar organizers from the basal land plant

356   Marchantia polymorpha. *New Phytologist* 209:999–1013. DOI: 10.1111/nph.13691.

357   Era A., Tominaga M., Ebine K., Awai C., Saito C., Ishizaki K., Yamato KT., Kohchi T., Nakano
358   A., Ueda T. 2009. Application of lifeact reveals F-actin dynamics in arabidopsis thaliana
359   and the liverwort, marchantia polymorpha. *Plant and Cell Physiology* 50:1041–1048. DOI:
360   10.1093/pcp/pcp055.

361   Gabryś H. 2004. Blue light-induced orientation move ments of chloroplasts in higher plants:
362   Recent progress in the study of their mechanisms. 26:473–478.

363   Hardham AR., Gunning BES. 1978. Structure of cortical microtubule arrays in plant cells. *J. Cell
364   Biol*:14–34.

365   Holzinger A., Buchner O., Lütz C., Hanson MR. 2007. Temperature-sensitive formation of
366   chloroplast protrusions and stromules in mesophyll cells of Arabidopsis thaliana.
367   *Protoplasma* 230:23–30. DOI: 10.1007/s00709-006-0222-y.

368   Ishizaki K., Nishihama R., Ueda M., Inoue K., Ishida S., Nishimura Y., Shikanai T., Kohchi T.
369   2015a. Development of gateway binary vector series with four different selection markers
370   for the liverwort Marchantia polymorpha. *Plos One* 10:e0138876. DOI:
371   10.1371/journal.pone.0138876.

372   Ishizaki K., Nishihama R., Yamato KT., Kohchi T. 2015b. Molecular genetic tools and
373   techniques for Marchantia polymorpha research. *Plant & cell physiology* 3:1532. DOI:
374   10.1093/pcp/pcv097.

375   Kadota A., Yamada N., Suetsugu N., Hirose M., Saito C., Shoda K., Ichikawa S., Kagawa T.,
376   Nakano A., Wada M. 2009. Short actin-based mechanism for light-directed chloroplast
377   movement in Arabidopsis. *Proceedings of the National Academy of Sciences of the United
378   States of America* 106:13106–11. DOI: 10.1073/pnas.0906250106.

379   Kagawa T., Wada M. 1996. Phytochrome- and blue-light-absorbing pigment-mediated
380   directional movement of chloroplasts in dark-adapted prothallial cells of fern Adiantum as
381   analyzed by microbeam irradiation. *Planta* 198:488–493. DOI: 10.1007/BF00620067.

382   Kandasamy MK., Meagher RB. 1999. Actin-organelle interaction: Association with chloroplast
383   in Arabidopsis leaf mesophyll cells. *Cell Motility and the Cytoskeleton* 44:110–118. DOI:
384   10.1002/(SICI)1097-0169(199910)44:2<110::AID-CM3>3.0.CO;2-O.

385   Kodama Y., Tsuboi H., Kagawa T., Wada M. 2008. Low temperature-induced chloroplast
386   relocation mediated by a blue light receptor, phototropin 2, in fern gametophytes. *Journal of
387   Plant Research* 121:441–448. DOI: 10.1007/s10265-008-0165-9.

388   Kodama Y. 2016. Time gating of chloroplast autofluorescence allows clearer fluorescence
389   imaging in planta. *PLOS ONE* 11:e0152484. DOI: 10.1371/journal.pone.0152484.
390   Komatsu A., Terai M., Ishizaki K., Suetsugu N., Tsuboi H., Nishihama R., Yamato KT., Wada
391   M., Kohchi T. 2014. Phototropin encoded by a single-copy gene mediates chloroplast
392   photorelocation movements in the liverwort Marchantia polymorpha. *Plant Physiology*
393   166:411–427. DOI: 10.1104/pp.114.245100.
394   Kong S-G., Arai Y., Suetsugu N., Yanagida T., Wada M. 2013. Rapid severing and motility of
395   chloroplast-actin filaments are required for the chloroplast avoidance response in
396   Arabidopsis. *The Plant cell* 25:572–90. DOI: 10.1105/tpc.113.109694.
397   Kong SG., Wada M. 2011. New insights into dynamic actin-based chloroplast photorelocation
398   movement. *Molecular Plant* 4:771–781. DOI: 10.1093/mp/ssr061.
399   Kost B., Spielhofer P., Chua NH. 1998. A GFP-mouse talin fusion protein labels plant actin
400   filaments in vivo and visualizes the actin cytoskeleton in growing pollen tubes. *Plant
401   Journal* 16:393–401. DOI: 10.1046/j.1365-313X.1998.00304.x.
402   Malec P., Rinaldi RA., Gabryś H. 1996. Light-induced chloroplast movements in Lemna trisulca.
403   Identification of the motile system. *Plant Science* 120:127–137. DOI: 10.1016/S0168-
404   9452(96)04506-2.
405   Ogasawara Y., Ishizaki K., Kohchi T., Kodama Y. 2013. Cold-induced organelle relocation in
406   the liverwort Marchantia polymorpha L. *Plant, Cell and Environment* 36:1520–1528. DOI:
407   10.1111/pce.12085.
408   Oikawa K., Matsunaga S., Mano S., Kondo M., Yamada K., Hayashi M., Kagawa T., Kadota A.,
409   Sakamoto W., Higashi S., Watanabe M., Mitsui T., Shigemasa A., Iino T., Hosokawa Y.,
410   Nishimura M. 2015. Physical interaction between peroxisomes and chloroplasts elucidated
411   by in situ laser analysis. *Nature Plants* 1:15035. DOI: 10.1038/nplants.2015.35.
412   Riedl J., Crevenna AH., Kessenbrock K., Yu JH., Neukirchen D., Bista M., Bradke F., Jenne D.,
413   Holak TA., Werb Z., Sixt M., Wedlich-Soldner R. 2008. Lifeact: a versatile marker to
414   visualize F-actin. *Nature methods* 5:605–7. DOI: 10.1038/nmeth.1220.
415   Sato Y., Wada M., Kadota A. 2001. Choice of tracks, microtubules and/or actin filaments for
416   chloroplast photo-movement is differentially controlled by phytochrome and a blue light
417   receptor. *Journal of Cell Science* 114:269–279.
418   Senn G. 1908. *Die gestalts-und lageveränderung der pflanzen-chromatophoren*. Leipzig:
419   Wilhelm-Engelmann.

420   Suetsugu N., Kagawa T., Wada M., Corporation T. 2005. An auxilin-like J-domain protein ,
421   JAC1 , regulates phototropin-mediated chloroplast movement. 139:151–162. DOI:
422   10.1104/pp.105.067371.flowering.

423   Suetsugu N., Higa T., Gotoh E., Wada M. 2016. Light-induced movements of chloroplasts and
424   nuclei are regulated in both cp-actin-filament-dependent and -independent manners in
425   Arabidopsis thaliana. *Plos One* 11:e0157429. DOI: 10.1371/journal.pone.0157429.

426   Suetsugu N., Wada M. 2007. Chloroplast photorelocation movement mediated by phototropin
427   family proteins in green plants. *Biological Chemistry* 388:927–935. DOI:
428   10.1515/BC.2007.118.

429   Tsuboi H., Wada M. 2012. Distribution pattern changes of actin filaments during chloroplast
430   movement in Adiantum capillus-veneris. *Journal of Plant Research* 125:417–428. DOI:
431   10.1007/s10265-011-0444-8.

432   Tsuboyama S., Kodama Y. 2014. AgarTrap: A simplified Agrobacterium-mediated
433   transformation method for sporelings of the liverwort Marchantia polymorpha L. *Plant and*
434   *Cell Physiology* 55:229–236.

435   Tsuboyama-Tanaka S., Kodama Y. 2015. AgarTrap-mediated genetic transformation using intact
436   gemmae/gemmalings of the liverwort Marchantia polymorpha L. *Journal of Plant Research*
437   128:337–344. DOI: 10.1007/s10265-014-0695-2.

438   Tsuboyama-Tanaka S., Nonaka S., Kodama Y. 2015. A highly efficient AgarTrap method for
439   genetic transformation of mature thalli of the liverwort Marchantia polymorpha L. *Plant*
440   *Biotechnology*:1–4. DOI: 10.5511/plantbiotechnology.15.0813a.

441   Wada M., Suetsugu N. 2004. Plant organelle positioning. *Current Opinion in Plant Biology*
442   7:626–631. DOI: 10.1016/j.pbi.2004.09.005.

443   Wagner G., Haupt W., Laux   a. 1972. Reversible inhibition of chloroplast movement by
444   cytochalasin B in the green alga mougeofia. *Science (New York, N.Y.)* 176:808–809. DOI:
445   10.1126/science.176.4036.808.

446   Yamashita H., Sato Y., Kanegae T., Kagawa T., Wada M., Kadota A. 2011. Chloroplast actin
447   filaments organize meshwork on the photorelocated chloroplasts in the moss Physcomitrella
448   patens. *Planta* 233:357–368. DOI: 10.1007/s00425-010-1299-2.

449

450

451   *Figure legends*

452   **Figure 1. Effect of inhibitors for actin filaments in organelle cold positioning.**

453   (a) Procedure of inhibitor treatments for actin filaments. (b) Representative images of chloroplast

454   position with the inhibitors, 1-µM latrunculin A (Lat) and 50-µM cytochalasin B (Cyto). As

455   controls, 1% ethanol (Et) and 0.25% DMSO were used. Chloroplast position was visualized with

456   chlorophyll fluorescence in red. Scale bar represents 50 µm. (c) Quantification of chloroplast

457   position (b) by measurement of the P/A ratio. Bars indicate standard deviations. (d)

458   Representative images of cold-mediated intracellular positions of nuclei at 5°C, with 1-µM

459   latrunculin A (Lat) as the inhibitor and 1% ethanol (Et) as a control. Scale bar represents 25 µm.

460   Lines are drawn along the cell shape. Fluorescence of Citrine-labeled nuclei (Ogasawara et al.,

461   2013) and chlorophyll were colored in green and red, respectively. (e) Representative images of

462   cold-mediated intracellular positions of peroxisomes at 5°C. Scale bar represents 25 µm. Lines

463   are drawn along the cell shape. Fluorescence of Citrine-labeled peroxisomes (Ogasawara et al.,

464   2013) and chlorophyll were colored in green and red, respectively.

465

466   **Figure 2. Effect of inhibitors for microtubules in organelle cold positioning.**

467   (a) Procedure of inhibitor treatments for microtubules. (b) Schematic illustration of Citrine-

468   MpTubulin. N and C indicate the amino and carboxyl termini, respectively. Bar represents 50

469   amino acids. (c) Disruption of microtubules visualized by Citrine-MpTubulin with 10-µM

470   oryzalin (Ory) treatment. Fluorescence of Citrine-MpTubulin and chlorophyll were colored in

471   yellow and red, respectively. Scale bars represent 25 µm. (d) Representative images of

472   chloroplast position with the inhibitor, 10-µM oryzalin (Ory). Scale bar represents 50 µm. (e)

473   Quantification of chloroplast position (d) by measurement of the P/A ratio. Bars indicate

474   standard deviations. (f) Representative images of cold-mediated intracellular positions of nuclei

475   and peroxisomes at 5°C, with 10-µM oryzalin (Ory) as the inhibitor. Scale bars represent 25 µm.

476   Lines are drawn along the cell shape. Fluorescence of Citrine-labeled organelles (nuclei and

477   peroxisomes) (Ogasawara et al., 2013) and chlorophyll were colored in green and red,

478   respectively. (g) Disruption of microtubules visualized by Citrine-MpTubulin at 5°C for 2 h.

479   Scale bars represent 10 µm. (h) Chloroplast positioning after treatment of 10-µM oryzalin (Ory)

480   at 22°C for 0 h, 2 h, or 24 h. Scale bar represents 50 µm.

481

482   **Figure 3. Lifeact-based visualization of actin filaments during chloroplast cold positioning.**

483   (a) Schematic illustration of Lifeact-Citrine. N and C indicate the amino and carboxyl termini,

484   respectively. Bar represents 50 amino acids. (b) Visualization of actin filaments mediated by

485   Lifeact-Citrine probe during chloroplast cold positioning in 1-day-old gemmaling. Fluorescence

486   of Lifeact-Citrine and chlorophyll were colored in yellow and red, respectively. Scale bars

487   represent 10 µm. (c) Visualization of actin filaments by Lifeact-Citrine probe in 4-day-old

488   gemmaling. Scale bar represents 10 µm. (d) Disruption of actin filaments visualized by Lifeact-

489   Citrine probe with treatment of 1-µM latrunculin A (Lat) and 50-µM cytochalasin B (Cyto).

490   Scale bars represent 10 µm.

491

492   **Figure 4. mTalin-based visualization of actin filaments during chloroplast cold positioning.**

493   (a) Schematic illustration of Citrine-mTalin. N and C indicate the amino and carboxyl termini,

494   respectively. Bar represents 50 amino acids. (b) Representative images of actin filaments

495   visualized by Citrine-mTalin during chloroplast cold positioning. Fluorescence of Citrine-mTalin

496   and chlorophyll were colored in yellow and red, respectively. Scale bars represent 10 µm. (c)

497   Disruption of actin filaments visualized by Citrine-mTalin with treatment of 1-µM latrunculin A

498   (Lat) and 50-µM cytochalasin B (Cyto). Scale bars represent 10 µm.

499

500   **Figure 5. Actin-dependency in the light-induced chloroplast positioning responses.**

501   (a) Procedure of inhibitor treatments to analyze chloroplast accumulation response. wBL, weak

502   blue-light. (b) Representative images of chloroplast position after induction of the accumulation

503   response with the inhibitor, 1-µM latrunculin A (Lat) or 10-µM oryzalin (Ory). As controls, 1%

504   ethanol (Et)   and 0.1 % DMSO were used.   Scale bar represents 50 µm. (c) Quantification of

505   chloroplast position (b) by measurement of the P/A ratio. Bars indicate standard deviations. (d)

506   Procedure of inhibitor treatments to analyze chloroplast avoidance response. wBL, weak blue-

507   light; sBL, strong blue-light. (e) Representative images of chloroplast position after induction of

508   the avoidance response with the inhibitor, Lat or Ory. As controls, 1% ethanol (Et)   and 0.1%

509   DMSO were used.   Scale bar represents 50 µm. (f) Quantification of chloroplast position (e) by

510   measurement of the P/A ratio. Bars indicate standard deviations.

Figure 1(on next page)

Effect of inhibitors for actin filaments in organelle cold positioning.

(a) Procedure of inhibitor treatments for actin filaments. (b) Representative images of chloroplast position with the inhibitors, 1-µM latrunculin A (Lat) and 50-µM cytochalasin B (Cyto). As controls, 1% ethanol (Et) and 0.25% DMSO were used. Chloroplast position was visualized with chlorophyll fluorescence in red. Scale bar represents 50 µm. (c) Quantification of chloroplast position (b) by measurement of the P/A ratio. Bars indicate standard deviations. (d) Representative images of cold-mediated intracellular positions of nuclei at 5°C, with 1-µM latrunculin A (Lat) as the inhibitor and 1% ethanol (Et) as a control. Scale bar represents 25 µm. Lines are drawn along the cell shape. Fluorescence of Citrine-labeled nuclei (Ogasawara et al., 2013) and chlorophyll were colored in green and red, respectively. (e) Representative images of cold-mediated intracellular positions of peroxisomes at 5°C. Scale bar represents 25 µm. Lines are drawn along the cell shape. Fluorescence of Citrine-labeled peroxisomes (Ogasawara et al., 2013) and chlorophyll were colored in green and red, respectively.

22°C   5°C
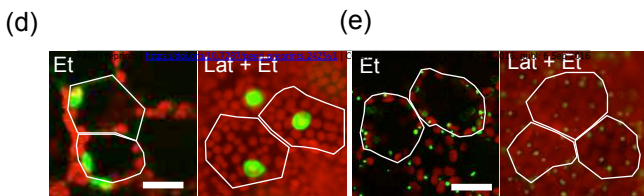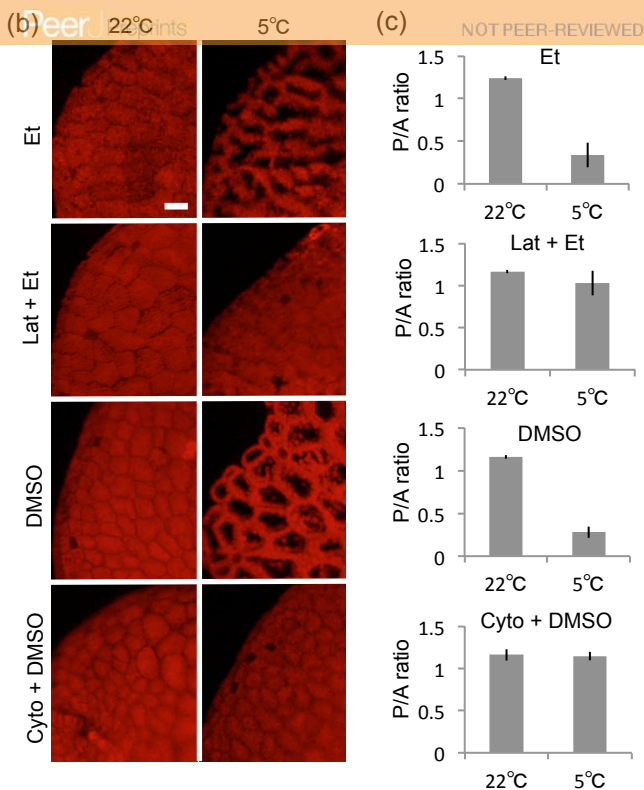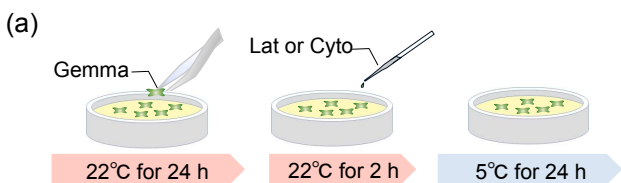
Figure 2(on next page)

Effect of inhibitors for microtubules in organelle cold positioning.

(a) Procedure of inhibitor treatments for microtubules. (b) Schematic illustration of Citrine-MpTubulin. N and C indicate the amino and carboxyl termini, respectively. Bar represents 50 amino acids. (c) Disruption of microtubules visualized by Citrine-MpTubulin with 10-µM oryzalin (Ory) treatment. Fluorescence of Citrine-MpTubulin and chlorophyll were colored in yellow and red, respectively. Scale bars represent 25 µm. (d) Representative images of chloroplast position with the inhibitor, 10-µM oryzalin (Ory). Scale bar represents 50 µm. (e) Quantification of chloroplast position (d) by measurement of the P/A ratio. Bars indicate standard deviations. (f) Representative images of cold-mediated intracellular positions of nuclei and peroxisomes at 5°C, with 10-µM oryzalin (Ory) as the inhibitor. Scale bars represent 25 µm. Lines are drawn along the cell shape. Fluorescence of Citrine-labeled organelles (nuclei and peroxisomes) (Ogasawara et al., 2013) and chlorophyll were colored in green and red, respectively. (g) Disruption of microtubules visualized by Citrine-MpTubulin at 5°C for 2 h. Scale bars represent 10 µm. (h) Chloroplast positioning after treatment of 10-µM oryzalin (Ory) at 22°C for 0 h, 2 h, or 24 h. Scale bar represents 50 µm.
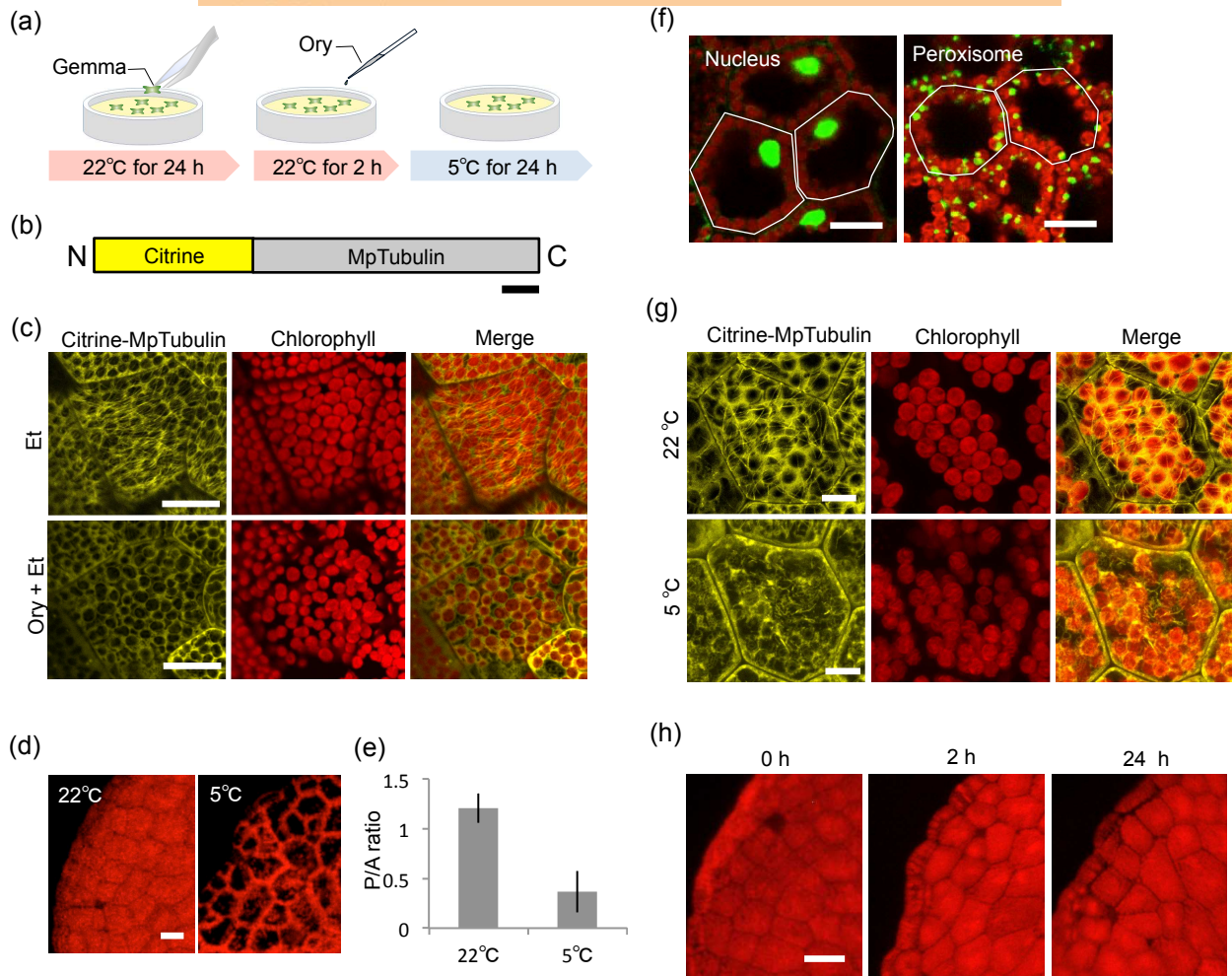
(a)

Gemma

Ory

22°C for 24 h   22°C for 2 h   5°C for 24 h

(b)

N   Citrine   MpTubulin   C

(f)

Nucleus   Peroxisome

(c)

Citrine-MpTubulin   Chlorophyll   Merge

Et

Ory + Et

(g)

Citrine-MpTubulin   Chlorophyll   Merge

22 °C

5 °C

(d)

22°C   5°C

(e)

P/A ratio

22°C   5°C

(h)

0 h   2 h   24 h

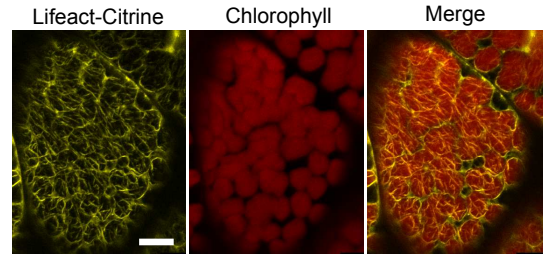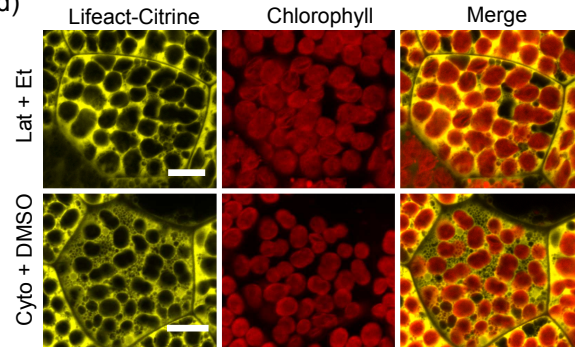**Figure 3**(on next page)

Lifeact-based visualization of actin filaments during chloroplast cold positioning.

(a) Schematic illustration of Lifeact-Citrine. N and C indicate the amino and carboxyl termini, respectively. Bar represents 50 amino acids. (b) Visualization of actin filaments mediated by Lifeact-Citrine probe during chloroplast cold positioning in 1-day-old gemmaling. Fluorescence of Lifeact-Citrine and chlorophyll were colored in yellow and red, respectively. Scale bars represent 10 µm. (c) Visualization of actin filaments by Lifeact-Citrine probe in 4-day-old gemmaling. Scale bar represents 10 µm. (d) Disruption of actin filaments visualized by Lifeact-Citrine probe with treatment of 1-µM latrunculin A (Lat) and 50-µM cytochalasin B (Cyto). Scale bars represent 10 µm.
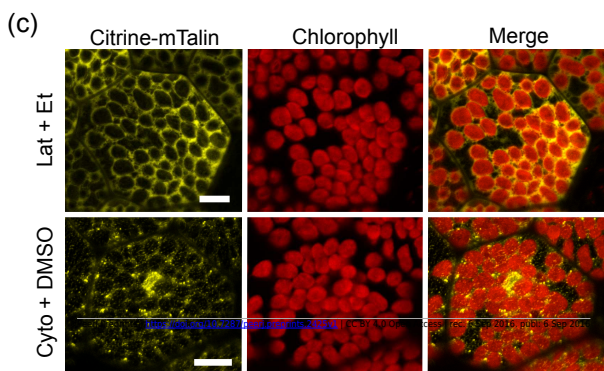
(a)
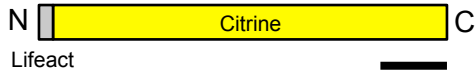
(b)
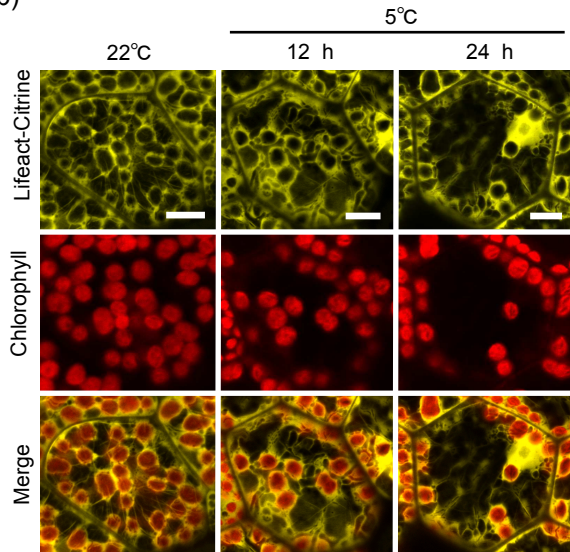
(c)

(d)

Figure 4(on next page)

mTalin-based visualization of actin filaments during chloroplast cold positioning.

(a) Schematic illustration of Citrine-mTalin. N and C indicate the amino and carboxyl termini, respectively. Bar represents 50 amino acids. (b) Representative images of actin filaments visualized by Citrine-mTalin during chloroplast cold positioning. Fluorescence of Citrine-mTalin and chlorophyll were colored in yellow and red, respectively. Scale bars represent 10 μm. (c) Disruption of actin filaments visualized by Citrine-mTalin with treatment of 1-μM latrunculin A (Lat) and 50-μM cytochalasin B (Cyto). Scale bars represent 10 μm.
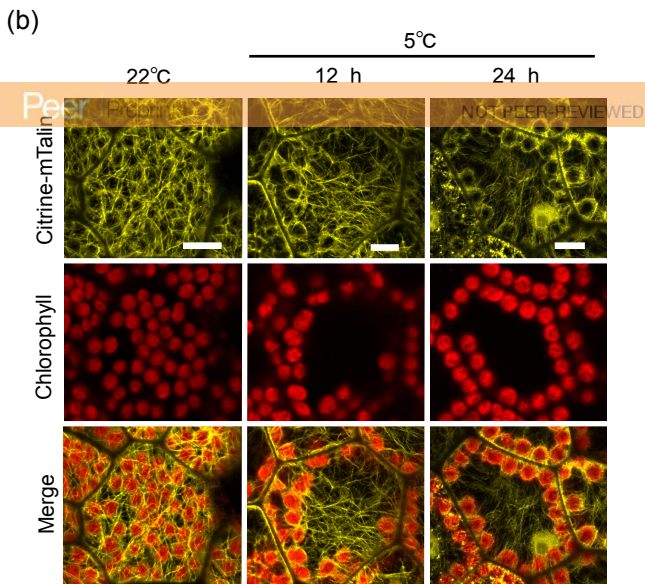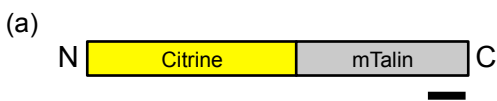
(a) N — Citrine — mTalin — C

(b)
	22°C	5°C 12 h	5°C 24 h
Citrine-mTalin			
Chlorophyll			
Merge			

(c)
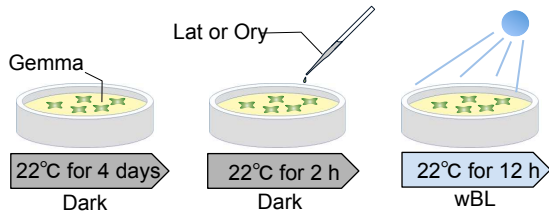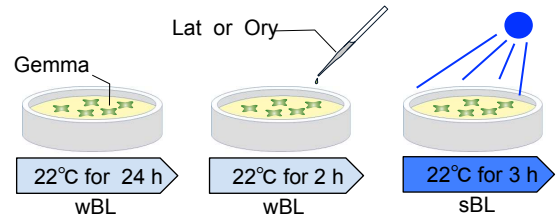|	Citrine-mTalin	Chlorophyll	Merge
Lat + Et			
Cyto + DMSO			

Figure 5(on next page)

Actin-dependency in the light-induced chloroplast positioning responses.

(a) Procedure of inhibitor treatments to analyze chloroplast accumulation response. wBL, weak blue-light. (b) Representative images of chloroplast position after induction of the accumulation response with the inhibitor, 1-µM latrunculin A (Lat) or 10-µM oryzalin (Ory). As controls, 1% ethanol (Et) and 0.1 % DMSO were used. Scale bar represents 50 µm. (c) Quantification of chloroplast position (b) by measurement of the P/A ratio. Bars indicate standard deviations. (d) Procedure of inhibitor treatments to analyze chloroplast avoidance response. wBL, weak blue-light; sBL, strong blue-light. (e) Representative images of chloroplast position after induction of the avoidance response with the inhibitor, Lat or Ory. As controls, 1% ethanol (Et) and 0.1% DMSO were used. Scale bar represents 50 µm. (f) Quantification of chloroplast position (e) by measurement of the P/A ratio. Bars indicate standard deviations.
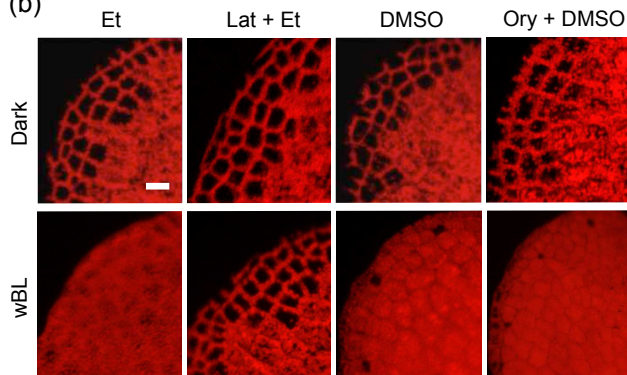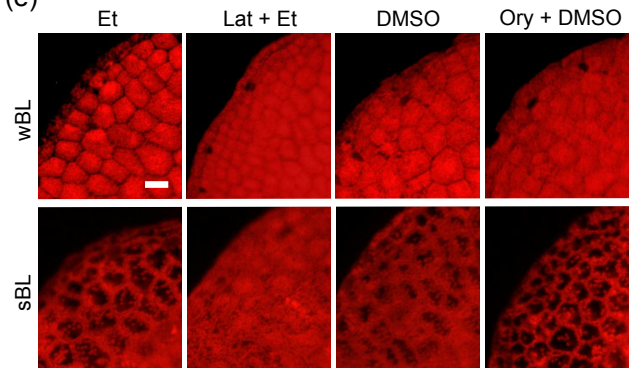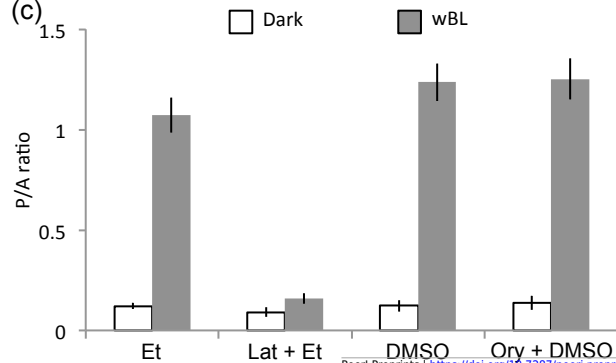
(a)
Gemma
Lat or Ory

22℃ for 4 days — Dark
22℃ for 2 h — Dark
22℃ for 12 h — wBL

(b)

| | Et | Lat + Et | DMSO | Ory + DMSO |

Dark

wBL

(c)

□ Dark   ■ wBL

P/A ratio

Et   Lat + Et   DMSO   Ory + DMSO

(d)
Gemma
Lat or Ory

22℃ for 24 h — wBL
22℃ for 2 h — wBL
22℃ for 3 h — sBL

(e)

| | Et | Lat + Et | DMSO | Ory + DMSO |

wBL

sBL

(f)

□ wBL   ■ sBL

P/A ratio

Et   Lat + Et   DMSO   Ory + DMSO